

Supplementary Information for:
Controlling Cellular Uptake of Nanoparticles
with pH-Sensitive Polymers

Hong-ming Ding¹ & Yu-qiang Ma^{1,2,*}

¹ *National Laboratory of Solid State Microstructures and Department of Physics,
Nanjing University, Nanjing 210093, China*

² *Center for Soft Condensed Matter Physics and Interdisciplinary Research,
Soochow University, Suzhou 215006, China*

* *E-mail address: myqiang@nju.edu.cn*

I. Supplementary Methods

The DPD is a coarse-grained simulation technique with hydrodynamic interaction¹. The dynamics of the elementary units which are so-called DPD beads, is governed by Newton's equation of motion $d\mathbf{v}_i/dt = \mathbf{f}_i/m$. Typically, in the DPD, there are three types of pairwise forces acting on bead i by bead j : the conservative force, dissipative force, and random force. In the present work, the electrostatic force is introduced to take into account the electrostatic interactions between charged beads. The conservative force $\mathbf{F}_{ij}^C = a_{ij}(1 - r_{ij}/r_c)\hat{\mathbf{e}}_{ij}$ is used to model the repulsive interaction of beads i and j , where $r_{ij} = |\mathbf{r}_{ij}|$ is the distance between beads i and j , $\hat{\mathbf{e}}_{ij} = \mathbf{r}_{ij}/r_{ij}$ is the unit vector, r_c is the cutoff radius of the force, and a_{ij} represents the maximum repulsion interaction of beads i and j . For any two beads of the same type, we take the repulsive parameter $a_{ii} = 25$, and for any two beads of different types, we set the interaction parameter $a_{WH} = a_{WP} = a_{WI} = a_{WC} = a_{HP} = a_{HI} = a_{HC} = a_{PI} = a_{PC} = a_{IC} = 25$ and $a_{WT} = a_{PT} = a_{HT} = a_{IT} = a_{CT} = 100$ (W stands for water bead, and I represents counterion bead which is introduced into the system to ensure the charge neutrality) to denote the hydrophilic/hydrophobic property of the beads^{2,3}. The dissipative force $\mathbf{F}_{ij}^D = -\gamma(1 - r_{ij}/r_c)(\hat{\mathbf{e}}_{ij} \cdot \mathbf{v}_{ij})\hat{\mathbf{e}}_{ij}$ and random force $\mathbf{F}_{ij}^R = \sqrt{2\gamma k_B T}(1 - r_{ij}/r_c)\zeta_{ij}\Delta t^{-1/2}\hat{\mathbf{e}}_{ij}$ are for thermostat, where $\mathbf{v}_{ij} = \mathbf{v}_i - \mathbf{v}_j$ is relative velocity between beads i and j , γ is the strength of friction, ζ_{ij} is a symmetric random variable with zero mean and unit variance, and Δt is the time step of simulation¹.

Electrostatic interactions were incorporated into the DPD simulations by Groot⁴. Since soft potential in the DPD allows for the overlap between DPD beads, when the charged DPD beads are modeled, this can lead to the formation of artificial ion pairs and cause the divergence of the electrostatic potential. To avoid this problem, Groot chose to spread out the charges using the distribution⁴: $\rho_e(r) = \frac{3}{\pi r_e^3}(1 - r/r_e)$ with $r < r_e$, where r_e is the electrostatic smearing radius, and is typically set as $1.6r_c$ (for details of the method, see Ref. 4).

Moreover, in order to mimic the receptor-ligand interaction, we use a modified LJ potential⁵: $U_{ij}^{LJ} = 4\epsilon[(\frac{\sigma}{r_{ij}})^{12} - (\frac{\sigma}{r_{ij}})^6] + 0.22\epsilon$, where $r_{ij} \leq r_{cut}$, $\sigma = 0.624r_c$, and ϵ is used to identify the strength of the receptor-ligand interaction (we fix it as $10 k_B T$). The cutoff r_{cut} of the potential is the same as that in the DPD (i.e., r_c) unless otherwise stated. Additionally, to guarantee the proper running of the DPD technology, the repulsive force is set to be $25k_B T/r_{cut}$ if it is larger than $25k_B T/r_{cut}$, therefore this potential becomes “soft”.

Further, we use a harmonic bond $U_s = k_s(1 - r_{i,i+1}/l_0)^2$ (here we choose $k_s = 64$, $l_0 = 0.5r_c$) between the neighboring beads to ensure the integrality of lipids and polymers, and insert a weaker bond ($k_s = 10$, $l_0 = 0.5r_c$) between the first hydrophobic beads on two tails of the lipid to keep the tails oriented in the same direction³. We also use a three-body bond angle potential $U_a = k_a(1 - \cos(\phi - \phi_0))$ to depict the rigidity of lipid tails ($k_a = 10$, $\phi_0 = 180^\circ$).

Our simulations apply the velocity-Verlet integration algorithm and the integration time step $\Delta t = 0.015\tau$. In addition, we choose the cutoff radius r_c , bead mass m , energy $k_B T$ as the simulation units. All simulations are performed in the NVT ensembles. The size of the simulation box is $65r_c \times 65r_c \times 40r_c$ with the number density of $\rho = 3/r_c^3$. The area (A_0) per lipid when the membrane is under zero tension at the beginning of the simulations is about $1.28nm^2$. During the simulations, to keep the membrane surface under zero tension, the box shape changes with the area (A_b) per lipid on the boundary, i.e., if $A_b > A_0$, the box will be compressed in X-Y plane until $A_b = A_0$; while if $A_b < A_0$, the box will be stretched in X-Y plane until $A_b = A_0$. At the same time, the box length in membrane-normal direction will change correspondingly to keep the box volume fixed². And we perform the above operation every 1000 time steps. The periodic boundary conditions are adopted in three directions. We can convert the DPD units into SI units via examining the membrane thickness and the lipid diffusion coefficient⁵. Usually, the thickness of DPPC bilayer is about 4nm and

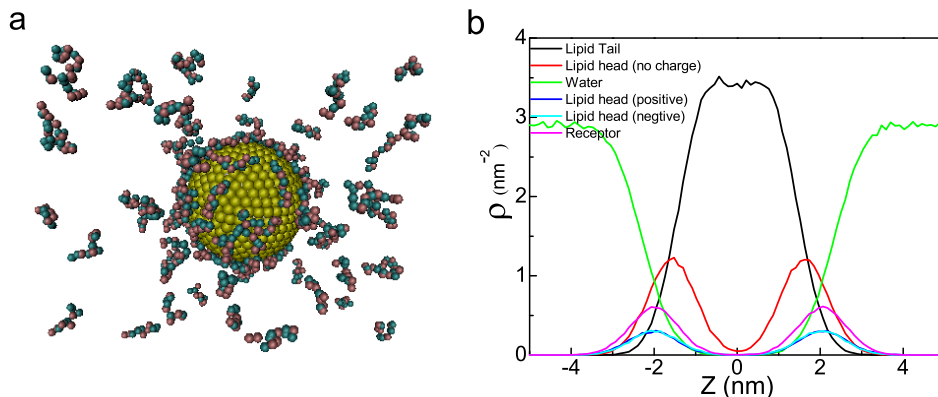


Figure S1: Additional information of nanoparticle-polymer solutions and membranes-water systems. (a) Snapshot of the initial state of placing nanoparticle in polymer solutions, where there are 100 polymers (the water and counterion beads are omitted). (b) Density profiles of water beads, lipid head beads, lipid tail beads and receptor head beads.

the in-plane diffusion constant of lipids is about $5.0\mu m^2/s$ in experiment. Comparing that the thickness is about $4.0r_c$ (the distance between two peaks in density profiles describing the first two beads of lipid molecules) and diffusion constant is about $0.012r_c^2/\tau$, we can yield $r_c = 1.0nm$ and $\tau = 2.4ns$. All simulations in this work are carried out by using the modified soft package Lammmps (12 Jun 2011)⁶.

II. Supplementary Figures and Discussions

Figures S2a-d show the snapshots of the final equilibrium of nanoparticle-polymers complex (NPC) under different ionized degrees (i.e., external pH value). With the increase of ionized monomer number, the electrostatic attractive interaction becomes stronger, and the number of adsorbed polymers on the nanoparticle will increase. However, with a further increase of ionized monomer number, the number of adsorbed polymers will decrease, i.e., the maximum number of adsorbed polymers corresponds to the middle range of N (from 4 to 6), as shown in Fig. S2e. This is due to an increase of the electrostatic repulsive interaction between the adsorbed polymers on the particle surface with ionized monomer number N , while the averaged attractive interaction energy be-

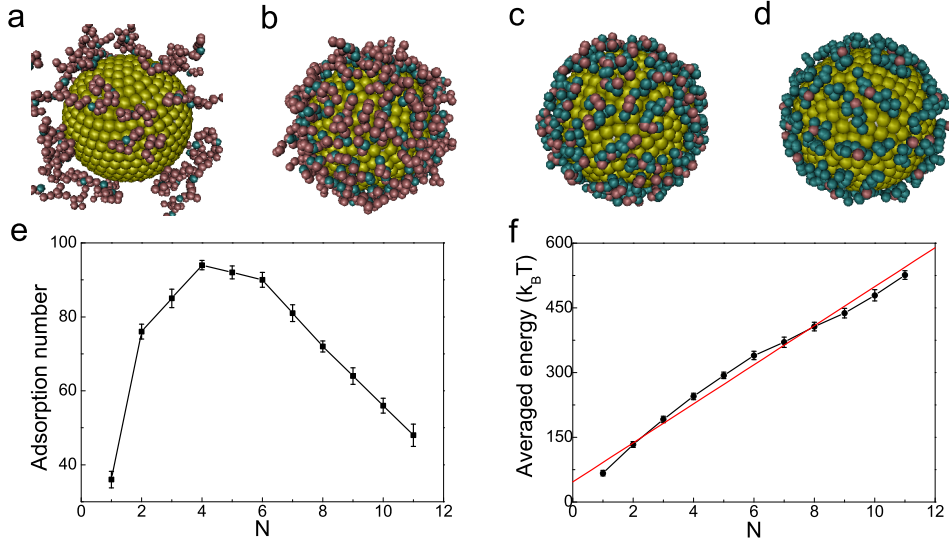


Figure S2: Final equilibrium of charged nanoparticles in polymer solutions. (a) $N=1$, (b) $N=4$, (c) $N=8$, and (d) $N=11$. The bead colors are the same as those of the snapshot in Fig. 1 in the main text. (e) The total adsorption number of polymers on the nanoparticles surface as a function of ionized number N . (f) The averaged attractive interaction energy (absolute value) between nanoparticles and polymers increase monotonously with ionized number N , indicating that the adsorbed polymers on the nanoparticle surface become more and more stable. The red line is the linear fitted line. Error bars are obtained by taking the standard derivation of ten independent simulations.

tween single polymer and nanoparticle increase linearly with the increase of N (see Fig. S2f).

In order to determine the zeta potential ζ of the nanoparticle-polymer complex, we first calculate the mean electrostatic potential ϕ at the distance r from the nanoparticle center⁷: $\phi(r) = \int_r^\infty dr' E(r') = \frac{q}{4\pi\epsilon} \int_r^\infty dr' \frac{P(r')}{r'^2}$, where $E(r)$ is the electric field and $P(r)$ is the integrated charge in units of q within the distance r , and ϵ is the dielectric constant of water. The mean electrostatic potential as functions of the distance r under different pH conditions is shown in Fig. S3. Then we can obtain the zeta potential in various cases. Interestingly, as shown in the inset of Fig. S3, it is found that the zeta potential will drop below zero when $N \geq 6$, indicating that the surface charge sign of nanoparticle could be changed because of

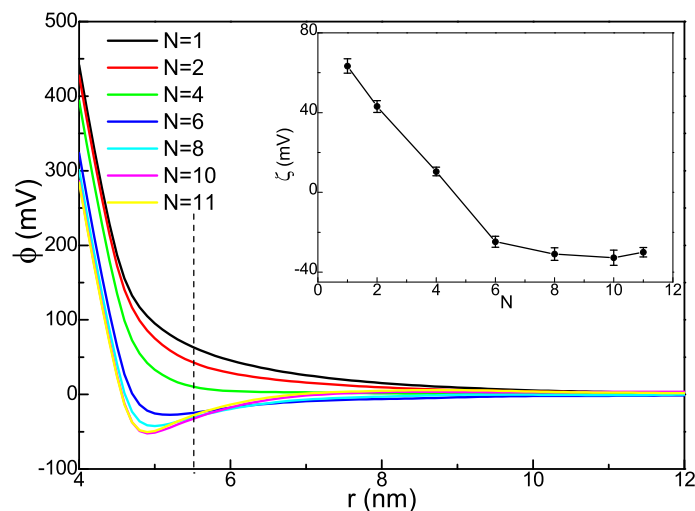


Figure S3: Mean electrostatic potential (ϕ) as a function of distance (r) from nanoparticle center. The inset shows the zeta potential (ζ) of nanoparticle-polymer complex as a function of the ionized number N . Note that the zeta potential cannot be obtained exactly in simulations because the shear plane is not easy to be determined⁷, here we just use the electrostatic potential corresponding to $r=5.5$ nm as the zeta potential⁸. Error bars are obtained by taking the standard derivation of ten independent simulations.

the associated anionic polymers on its surface.

Supplementary References

- ¹ Groot, R. D. & Warren, P. B. Dissipative particle dynamics: Bridging the gap between atomistic and mesoscopic simulations. *J. Chem. Phys.* **107**, 4423-4435 (1997).
- ² Smith, K. A., Jasnow, D. & Balazs, A. C. Designing synthetic vesicles that engulf nanoscopic particles. *J. Chem. Phys.* **127**, 084703 (2007).
- ³ Ding, H. M., Tian, W. D. & Ma, Y. Q. Designing nanoparticle translocation through membranes by computer simulations. *ACS Nano* **6**, 1230-1238 (2012).
- ⁴ Groot, R. D. Electrostatic interactions in dissipative particle dynamics — simulation of poly-electrolytes and anionic surfactants. *J. Chem. Phys.* **118**, 11265 (2003).

- ⁵ Yang, K. & Ma, Y. Q. Computer simulation of the translocation of nanoparticles with different shapes across a lipid bilayer. *Nat. Nanotechnol.* **5**, 579-583 (2010).
- ⁶ Plimpton, S. J. Fast parallel algorithms for short-range molecular dynamics. *J. Comput. Phys.* **117**, 1-19 (1995).
- ⁷ Diehl, A. & Levin, Y. Smoluchowski equation and the colloidal charge reversal. *J. Chem. Phys.* **125**, 054902 (2006).
- ⁸ Wang, Z. Y. & Ma, Y. Q. Insights from Monte Carlo simulations on charge inversion of planar electric double layers in mixtures of asymmetric electrolytes. *J. Chem. Phys.* **133**, 064704 (2010).